International Journal of Modern Manufacturing Technologies
ISSN 2067–3604, Vol. XV, No. 3 / 2023
https://doi.org/ 10.54684/ijmmt.2023.15.3.199

OPTIMIZATION OF HYDRAULIC DRIVES FOR SYNCHRONIZING WORKING MOVEMENTS OF AUTOMATED BRICK PRODUCTION INSTALLATION

Viacheslav Perepelytsia[1], Leonid Kozlov[1], Iurii Buriennikov[1], Nataliia Burennikova[1], Sergii Kozlov[1], Oana Rusu[2], Ioan Rusu[2]

[1]Vinnytsia National Technical University, Khmelnytske Shose 95, Vinnytsia, 21021, Ukraine
[2]"Gheorghe Asachi" Technical University, 41 Dimitrie Mangeron Blvd., Iași, 700050, Romania

Corresponding author: Oana Rusu, oana.rusu@academic.tuiasi.ro

Abstract: The paper presents a version of the improved string cutting installation for forming bricks with two hydraulic drives. A mathematical model of the movement of the traverse and the carriage of the installation, which require synchronous actions in the process of work, has been compiled. The dependence of the total force of the technological load and friction acting on the traverse on the movement parameters and tool geometry was obtained experimentally. The obtained dependence was used in the development of a mathematical model, represented by a system of nonlinear differential equations that were solved by the Rosenbrock method. A complex criterion for evaluating the efficiency of the automatic installation was formed and the values of the structural parameters of hydraulic drives were found, in which the errors of the geometric dimensions of the products and the power consumption will be minimal, and the productivity of the installation will be maximal.
Key words: automatic brick forming machine, hydraulic drives, synchronization, mathematical model, complex criterion, optimization.

1. INTRODUCTION

Various systems for synchronization of several working movements are widely used in modern practice of automated design of hydraulically driven machines and mechanisms. Vast majority of such systems use tracking devices. For instance, authors in (Chen et al., 2008) provide synchronous positioning for a two-cylinder electro-hydraulic system. The system monitors both cylinders and generates the respective control signal. The performed simulation and experimental research demonstrated that such system can maintain tracking error of the synchronization deviation within the limits of double measurement resolution without modification of the structure and its components.
In work (He et al., 2016), a pile-driver with four hydraulic motors is suggested. The authors claim that the system can perform synchronization regardless of the installation weight. However, the installation's behaviour is unstable. The system must operate stably to ensure minimal synchronization deviation.
The study (Wos and Dindorf, 2015) aimed at creating a simplified manipulator system that would be able to counter factors that negatively affect synchronization of the entire system. The authors referred non-linear friction at low speeds, mechanical components elasticity, changes in the structure shape under the influence of external forces to such factors. This was achieved by using control system of a feedback manipulator measuring the manipulator position deviation.
Working elements of installations ensuring synchronization of working bodies can work under external forces of different magnitude and direction. These forces significantly affect dynamic features of the synchronization system. Under such conditions, synchronization of working elements' movement can be ensured by installing a liquid flow divider. In article (Rafa et al., 2014), a flow divider was used to control movement of two loaded drives. The authors claim that using a flow divider is a simple and cheap method of synchronization with sufficiently high accuracy.
Structure of an electro-hydraulic elevator system composed of a flow regulator with three proportional valves was suggested in work (Ke at al., 2001). A feedback control system is also used to regulate the elevator speed. The research result is achievement of movement deviation for two cylinders within 2 mm.
In article (Bushuev et al., 2018), a method for optimal design of multi-element synchronization systems is suggested. A hydraulic scheme for synchronizing several units of angular movement of working nodes with

throttle control devices was used.
In article (Yang and Jin, 2021), lifting speed with a given value is ensured and also smooth operation of each lifter are achieved for a hydraulic lifting system. For the system synthesis a model of a pressure compensator and a variable throttle element was selected. The obtained results improve stability and speed of the lifting process. In work (Teixeira et al, 2015) theoretical and experimental analysis of operation of a hydraulic brake press with synchronized cylinders, where movement of each of them is controlled by an independent variable-speed electric motor is represented. Such design has a number of advantages but it is important for the system to use double-acting cylinders with defined parameters. Analysis of dynamic features of hydraulic lifting system, selection of its parameters, and the rule for changing control signal are provided in work (Liu, 2015). In work (Kassem at al., 2012), it was established that during transient processes in the synchronization system of two hydraulic motors, due to the inertia of the spool valve of the flow divider, an error in the speed of movement of the hydraulic motors occurs, which can reach 43%. The possibility of reducing this error to 26% when using a two-slot throttling directional valve in the flow divider has been confirmed. In the article (Mikova et al., 2014), possible variants of synchronous lifting and lowering of heavy structures with the help of hydraulic drives are considered while meeting safety and accuracy requirements. Proposals have been developed for selecting a hydraulic system in accordance with the type and accuracy of hydraulic drives. The work (Jia and Li-jun, 2011) analyses the principle of operation of the hydraulic system for synchronizing the movement of the working bodies of the sheet metal bending machine. It was found that the mechanical feedback control system of the hydraulic synchronizing valve provides an accuracy of 0.15 mm of use. The article (Chun-Yu et al., 2010) considers the of use. The article (Chun-Yu et al., 2010) considers the with a fairly low cost of such a system and high ease synchronization of two coupled motors in a vibration system. For this, their dynamic model was created and the peculiarity of the synchronization of two connected engines is physically explained. It was found that the accuracy of the synchronization of such a system depends on the distance between the motors and the centre of mass of the vibrating system.
System of synchronizing movement speed of two hydraulic cylinders can be efficiently applied in automated installations for production of brick work pieces. In cases where external forces acting on the system change within narrow ranges, the system for synchronizing movement of two hydraulic cylinders can be created based on an adjustable throttle installed in the fluid supply line of each power cylinder (Bushuev et al., 2018). The task of creating a new scheme and design of an installation for forming brick workpieces and determining the optimal values of structural parameters that ensure maximum productivity with the required quality indicators of workpieces. and minimal power losses is urgent.

2. INSTALLATION FOR FORMING BRICK WORKPIECES

In Fig. 1 hydraulic scheme of the installation for forming brick workpieces developed by the authors is represented.

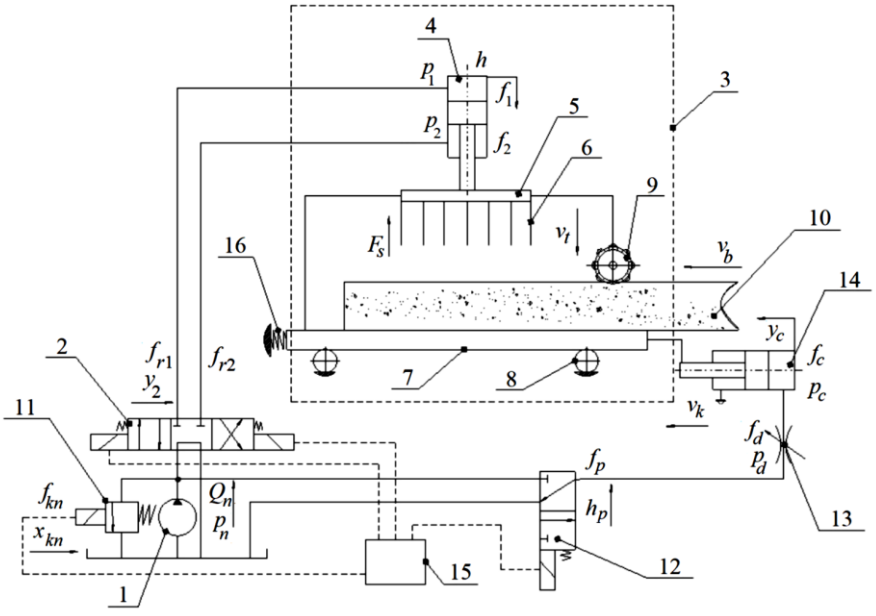

Fig 1. Hydraulic scheme of installation for forming brick workpieces

The installation includes: pump 1, directional valves with electromagnetic control 2 and 12, carriage 3, hydraulic cylinder of traverse 4, traverse 5, strings 6, table 7, rolling supports 8, motion sensor 9, clay bar 10, safety and overflow valve 11, directional valve 12, adjustable throttle 13, hydraulic cylinder of carriage 14, control unit 15, spring 16. The installation operates as follows. Clay bar 10 squeezed out of extruder moves along table 7 of carriage 3. Motion sensor 9 counts the size of n number of brick workpieces (depending on the number of strings 6) and sends an electrical signal to control unit 15. The latter generates control signals for safety and overflow valve 11 and directional valves 2 and 12. Working fluid from pump 1 is sent through distributor 2 to hydraulic cylinder of traverse 4 and through directional valve 12 to hydraulic cylinder of carriage 14. Hydraulic cylinder 4 drives traverse 5 with strings 6, for cutting the clay bar into workpieces. Hydraulic cylinder of carriage 14 ensures synchronization of movement speed of carriage 3 located on rolling supports 8, with movement speed of clay bar 10. During synchronous movement of clay bar 10 and carriage 3, the workpieces are cut. After the cutting cycle ends, spring 16 returns hydraulic cylinder of carriage 14 to the initial position.
A photo of the experimental installation for forming brick workpieces is presented in Fig. 2.

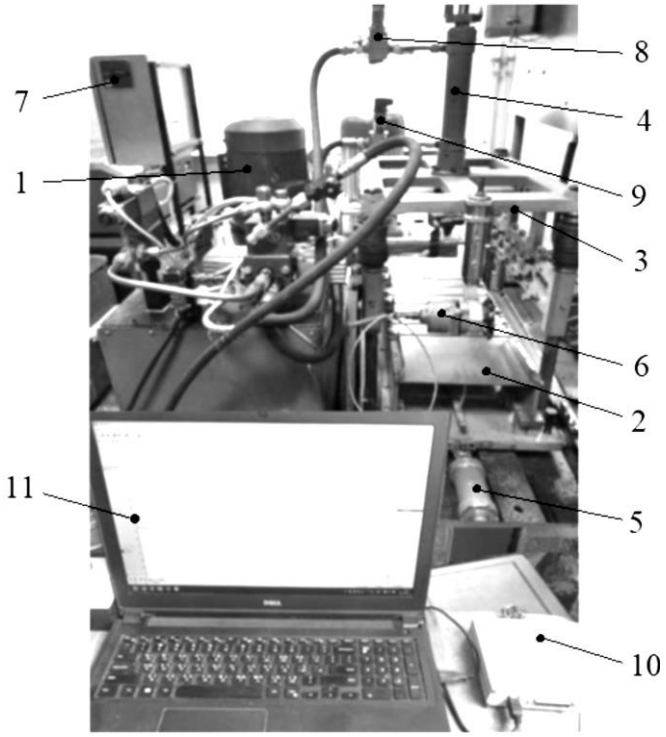

Fig. 2. Experimental installation for forming brick workpieces

Main nodes of experimental installation for forming brick workpieces are: pumping station 1; carriage 2; traverse 3 with strings; traverse hydraulic cylinder 4; carriage hydraulic cylinder 5; motion sensor 6; control unit 7; pressure sensors 8, 9 installed in piston and rod chambers of the traverse hydraulic cylinder, respectively; analogue to digital converter 10 (ADA-1406); personal computer 11.

3. RESEARCH METHODOLOGY

A mathematical model of the installation's hydraulic system was developed to study work processes during the formation of brick workpieces and determine the optimal design parameters. The mathematical model is built with the following basic simplifications and assumptions (Kozlov et al.,2019). Clay bar feed speed is taken as a constant value; concentrated parameters of the hydraulic drive elements are considered; temperature and viscosity of the working fluid do not change during one cutting cycle; fluid pressure in the drain lines is constant; pressure losses in hydraulic lines are not taken into account; working fluid flow in pump cracks and hydraulic cylinders are not taken into account.
Mathematical model of hydraulic drives of the installation for forming brick workpieces is a system of differential equations 1 – 10. It is marked in the mathematical model. Q_n – pump supply; μ – flow rate

coefficient; f_{kn}, f_1, f_2, f_p, f_{r1}, f_{r2}, f_d, f_c – areas of safety and overflow valve 11, piston and rod chambers of traverse hydraulic cylinder 4, directional valves 12 and 2, throttle 13 and hydraulic cylinder of carriage 14; ρ – working fluid density, p_n, p_1, p_2, p_d, p_c – pressures at pump outlet 1, inlet and outlet of traverse hydraulic cylinder 4, throttle outlet, inlet of carriage hydraulic cylinder 14; β_s – total coefficient of pliability of working fluid and rubber-metal pipelines, β – coefficient of working fluid pliability; W_n, W_1, W_2, W_d, W_c – volumes of pressure pipeline, flexible hose of piston and rod cavity of traverse hydraulic cylinder 4, flexible hose of throttle, carriage hydraulic cylinder 14; m_{kn}, m_2, m_p, m_t, m_c, m_k – weights of safety and overflow valve 11, directional valves 2 and 12, traverse 5, carriage hydraulic cylinder 14 and carriage 3; x_{kn} – stroke of spool of safety and overflow valve 11; c_x, c_2, c_p, c_c – stiffness of springs of safety and overflow valve 11, directional valves 2 and 12, springs of carriage 16; H_{kn}, H_2, H_p, H_c, – preceding compressions of springs of safety and overflow valve 11, springs of directional valves 2 and 12 and carriage 3; R_{rg} – hydrodynamic force; b_{kn}, b_2, b_p, b_c – coefficients of viscous friction of safety and overflow valve 11, directional valves 2 and 12, carriage hydraulic cylinder 14; y_2 – coordinate of directional valve 2 spool position; F_2, F_m – forces of electromagnets of directional valves 2 and 12; h – coordinate of traverse 5 position; F_s – traverse 5 load force; g – acceleration of free fall; y_c – coordinate of hydraulic cylinder 14 position; h_p – coordinate of directional valve 12 spool; v_b – clay bar speed.

$$Q_n = \mu f_{kn}\sqrt{\frac{2p_n}{\rho}} + \mu f_r\sqrt{\frac{2|p_n - p_1|}{\rho}}sign(p_n - p_1) + \mu f_p\sqrt{\frac{2|p_n - p_c|}{\rho}}sign(p_n - p_c) + \beta W_n\frac{dp_n}{dt}; \quad (1)$$

$$\mu f_{r1}\sqrt{\frac{2|p_n - p_1|}{\rho}}sign(p_n - p_1) = f_1\frac{dh}{dt} + \beta_s W_1\frac{dp_1}{dt}; \quad (2)$$

$$m_{kn}\frac{d^2x_{kn}}{dt^2} = p_n f_{kn} - c_x(H_{kn} + x_{kn}) - R_{rg} - b_{kn}\frac{dx_{kn}}{dt}; \quad (3)$$

$$m_2\frac{d^2y_2}{dt^2} = F_2 - c_2H_2 - b_2\frac{dy_2}{dt}; \quad (4)$$

$$m_t\frac{d^2h}{dt^2} = p_1f_1 - p_2f_2 - F_s^* + m_t g; \quad (5)$$

$$f_2\frac{dh}{dt} = \mu f_{r2}\sqrt{\frac{2p_2}{\rho}} + \beta_s W_2\frac{dp_2}{dt}; \quad (6)$$

$$\mu f_p\sqrt{\frac{2|p_n - p_d|}{\rho}}sign(p_n - p_d) = \mu f_d\sqrt{\frac{2|p_d - p_c|}{\rho}}sign(p_d - p_c) + \beta W_d\frac{dp_d}{dt}; \quad (7)$$

$$\mu f_d\sqrt{\frac{2|p_d - p_c|}{\rho}}sign(p_d - p_c) = f_c\frac{dy_c}{dt} + \beta_s W_c\frac{dp_c}{dt}; \quad (8)$$

$$m_p\frac{d^2h_p}{dt^2} = F_m - c_p\left(H_p + h_p\right) - b_p\frac{dh_p}{dt}; \quad (9)$$

$$(m_c + m_k)\frac{d^2y_c}{dt^2} = p_c f_c - c_c(H_c + y_c) + b_c\left(v_b - \frac{dy_c}{dt}\right). \quad (10)$$

The model research was carried out in MATLAB Simulink environment. Since the developed system of nonlinear differential equations is rigid, Rosenbrock numerical method was used to solve it with absolute accuracy ε_a=10^{-6} and relative accuracy $\varepsilon_в$=10^{-3}.

4. RESULTS AND DISSCUSSIONS

In the course of experiments, pressure sensors 8 and 9 were used to measure dependences of pressure values p_1 in the piston chamber and p_2 in the rod chamber of traverse hydraulic cylinder 4. Dependencies of pressure in the traverse hydraulic cylinder on time at different of the traverse speed values v_t are shown in figures 3 to 5.

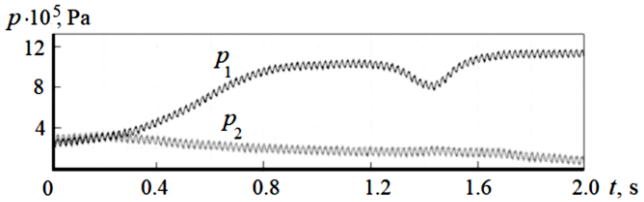

Fig. 3. Dependences of pressure values p_1 and p_2 in chambers of traverse hydraulic cylinder on time at v_t=0.2 m/s

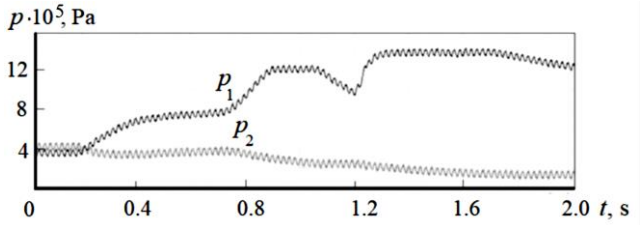

Fig. 4. Dependences of pressure values p_1 and p_2 in chambers of traverse hydraulic cylinder on time at v_t=0.3 m/s

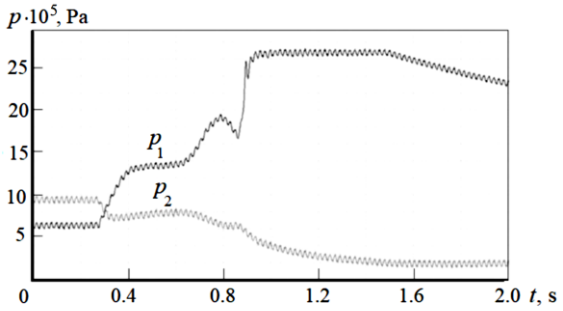

Fig. 5. Dependences of pressure values p_1 and p_2 in chambers of traverse hydraulic cylinder on time at v_t=0.4 m/s

Experiments were carried out with change in the traverse speed v_t at three levels and three values of string diameter d_s (Adler et al., 1976).
The total load force Fs was determined by formula:

$$F_s = p_1 \cdot f_1 - p_2 \cdot f_2 \tag{11}$$

where f_1, f_2 are areas of traverse hydraulic cylinder chambers. The calculation results were approximated using DataFit program and an equation of dependence of force F_s on traverse speed v_t and string diameter d_s was obtained, which was later used in mathematical model of hydraulic drives of the installation.

$$F_s^* = a + b \cdot d_s + c \cdot v_t + d \cdot d_s^2 + e \cdot v_t^2 + f \cdot d_s \cdot v_t \tag{12}$$

where a=3102.5, b=320.3, c=-16681.7, d=77.6, e=38505.6, f= -613.3, d_s is string diameter (mm), v_t is traverse speed (m/s). The experimental research results are shown in Table 1.

Table 1. Results of experimental research on determining the traverse load force

d_s, mm	v_t, m/s	F_s, N experiment No. 1	F_s, N experiment No. 2	F_s, N experiment No. 3	Average value F_s, N	Calculated value F_s^*, N
1.0	0.2	1567	1642	1601	1603	1581
	0.3	1734	1752	1764	1750	1777
	0.4	2767	2727	2753	2749	2743
1.5	0.2	1744	1705	1775	1742	1777
	0.3	1991	1998	1959	1982	1942
	0.4	2901	2805	2915	2874	2877
2.0	0.2	2025	1951	2103	2026	2011
	0.3	2117	2115	2169	2151	2146
	0.4	3085	2933	3131	3070	3050

In Fig. 6, dependence of the total traverse load force F_s* on traverse speed v_t and string diameter d_s is shown. Coefficient of determination for approximated dependence is R^2=0.993.
The major quality indicator of the manufactured brick is its size. The standard values are: width W = 250 mm, length L = 120 mm, height H = 65 mm. The installation for forming brick workpieces cuts a clay bar by height and therefore must ensure the size of H = 65 mm with the maximum possible deviation of δ_3 = 3 mm.
In order to achieve the highest accuracy of the workpiece, it is necessary that the installation carriage moves with the speed v_k as close as possible to the clay bar feed speed v_b during the entire cutting time. The accuracy of the production of the workpiece was estimated on the basis of the value δ, which depends on the difference between the speed of movement of the carriage v_k and the speed of movement of the beam v_b.

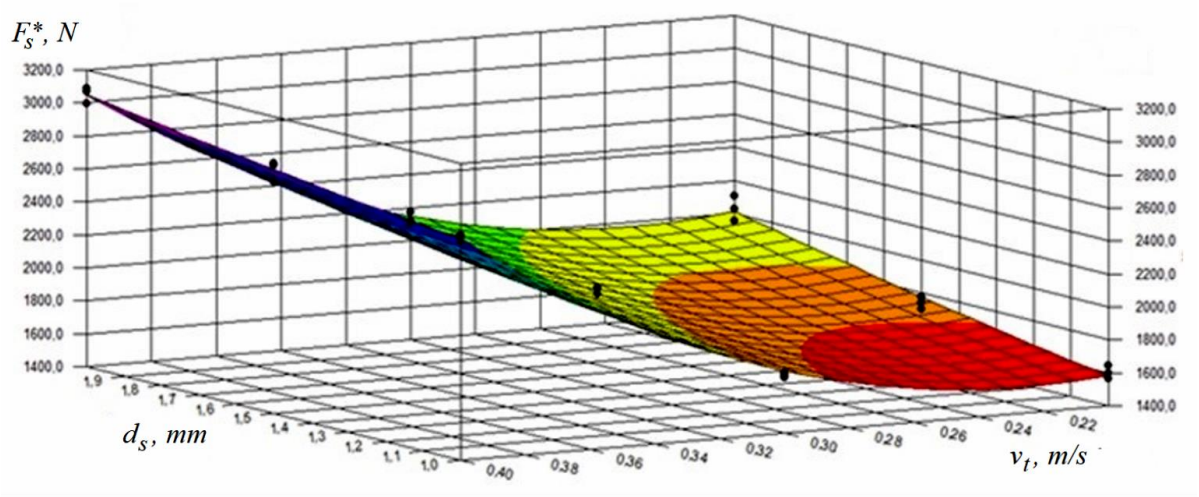

Fig. 6. Dependence of traverse load force F_s^* on values of v_t and d_s

The value of deviation δ was determined as the sum of modules of difference in the carriage and the clay bar movement speeds, from the beginning of cutting up to the end of the carriage movement with t_0 step.

$$\delta = \sum_1^n \frac{|v_k - v_b|}{t_0} \tag{13}$$

where t_0 =0.05 s.
The value of δ_3 of deviation of the workpiece's geometric shape. was determined by the formula:

$$\delta_3 = {}^{\delta}/_{H} \cdot 100\% \tag{14}$$

Based on dependence of carriage movement speed v_k on time, carriage movement deviation δ relative to the clay bar was determined defining geometric accuracy of the brick workpiece. Based on the mathematical model research parameters (Table 2) affecting the carriage movement deviation were determined.

Table 2. Influence of installation parameters on the carriage movement deviation

Installation parameters	Value (parameters range)	Units of measure	Impact on carriage movement deviation δ
f_d (throttle area)	(2...4) $\cdot 10^{-6}$	m^2	++
f_c (area of feeding hydraulic cylinder)	(10...30) $\cdot 10^{-4}$	m^2	++
m_c (weight of feeding hydraulic cylinder)	1...10	kg	0
W_c (volume of hydraulic cylinder)	(1...9) $\cdot 10^{-4}$	m^3	–
W_g (volume of flexible hose)	(0.5...5) $\cdot 10^{-4}$	m^3	–
m_k (weight of carriage)	50…300	kg	0
p_n (nominal pressure)	(20…50) $\cdot 10^5$	Pa	++
c_c (spring stiffness)	(1.5…3) $\cdot 10^4$	N/m	+
H_c (preliminary compression of spring)	0.01...0.06	m	+

The following symbols are introduced in Table 2: "++" – the parameter has strong effect (70 - 100% of the maximum value); "+" – the parameter has moderate effect (30 - 70%); "–" – the parameter has weak effect (5 - 30%); "0" – the parameter has no effect (up to 5%). Based on the data represented in Table 2, the main parameters affecting carriage movement deviation relative to the clay bar were determined: f_d – area of throttle 13 working window, f_c – area of carriage hydraulic cylinder 14 and p_n – nominal pressure of pump 1. Influence of the main parameters on carriage movement deviation relative to the clay bar is shown in Fig. 7. Values of the dimensionless parameters PR/PR_{max} are plotted on the abscissa axis, where PR are current parameter values and PR_{max} are maximum parameter values. The maximum values correspond to the upper limits of the parameter change ranges given in Table 2.

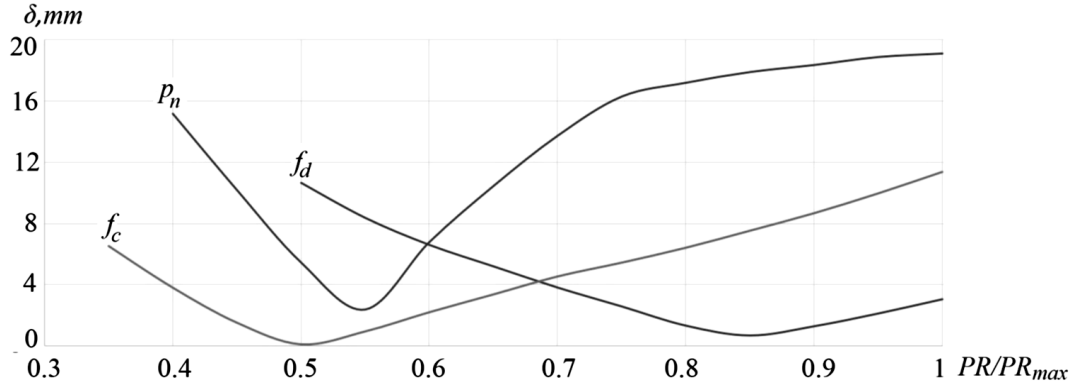

Fig. 7. Effect of brick forming installation parameters on δ

Major parameters f_d, f_c, p_n affect the installation efficiency in different ways. Selection of values of parameters f_d, f_c, p_n during the installation design was determined based on optimization. Optimization criterion (Kozlov et al, 2018) was determined as:

$$k = 0.5\frac{\delta}{\delta_{max}} - 0.3\frac{A}{A_{max}} + 0.2\frac{N}{N_{max}} \tag{15}$$

where δ – carriage movement deviation relative to the clay bar (mm), A – number of manufactured brick workpieces per hour (pcs/h), N – power losses on the safety and overflow valve (W); δ_{max}, A_{max}, N_{max} - maximum values of the carriage movement deviation, installation productivity and power losses on the overflow valve, determined in the optimization process.

The installation productivity A was determined as a fraction of length of the clay bar fed at the bar speed v_b per 1 hour, based on the size of one workpiece.

$$A = \frac{v_b \cdot 60 \cdot 60}{0.065} \tag{16}$$

Power losses N on the safety and overflow valve was determined as the product of pump consumption Q_n and pressure p_n at the pump outlet.

$$N = Q_n \cdot p_n \tag{17}$$

where $Q_n = 0.73 \cdot 10^{-3}$ m^3/s.

To carry out optimization, each of the parameters f_d, f_c, p_n was changed at three levels. 27 experiments were performed. Values of the optimization criterion were determined in each experiment. The combination of values of design parameters was considered optimal, in which the optimization criterion k has the smallest value. Maximum efficiency of the installation is achieved with optimization parameter values ensuring the minimum value of the optimization criterion. The research results are shown in Table 3.

In experiment No. 9, a combination of major parameters $f_c = 10 \cdot 10^{-4}$ m^2, $f_d = 4 \cdot 10^{-6}$ m^2 and $p_n = 40 \cdot 10^5$ Pa was found, at which deviation of the workpiece's geometric shape δ_3 =1,88 %, productivity A =6258 pcs/h, and lost power N=2920 W, which corresponds to the best value of the optimality criterion.

Table 3. Results of the research on determining optimization criterion

Exp. No.	$f_c \cdot 10^{-4}$, m^2	$f_d \cdot 10^{-6}$, m^2	$p_n \cdot 10^5$, Pa	$\delta \cdot 10^{-3}$, m	δ_3, %	A, pcs/h	N, W	k
1	10	2	20	8.32	12.8	1385	1460	0.491
2	10	2	30	2.31	3.5	2935	2190	0.136
3	10	2	40	1.2	1.85	3932	2920	0.077
4	10	3	20	8.6	13.25	1717	1460	0.490
5	10	3	30	2.67	4.1	3877	2190	0.111
6	10	3	40	1.16	1.8	5317	2920	0.009
7	10	4	20	9.1	14	1772	1460	0.515
8	10	4	30	2.64	4	4431	2190	0.083
9	**10**	**4**	**40**	**1.22**	**1.88**	**6258**	**2920**	**-0.033**
10	20	2	20	1.28	1.97	1717	1460	0.088
11	20	2	30	0.5	0.77	2326	2190	0.066
12	20	2	40	0.47	0.73	2825	2920	0.090
13	20	3	20	0.92	1.42	2492	1460	0.031
14	20	3	30	0.68	1.05	3378	2190	0.025
15	20	3	40	0.65	1	4098	2920	0.039
16	20	4	20	1.1	1.7	3157	1460	0.009
17	20	4	30	0.65	1	4320	2190	-0.021
18	20	4	40	0.43	0.66	5317	2920	-0.031
19	30	2	20	0.75	1.15	1329	1460	0.077
20	30	2	30	0.43	0.66	1717	2190	0.091
21	30	2	40	0.54	0.84	1994	2920	0.134
22	30	3	20	0.66	1	1938	1460	0.043
23	30	3	30	0.47	0.73	2492	2190	0.056
24	30	3	40	0.23	0.36	2991	2920	0.070
25	30	4	20	0.58	0.9	2548	1460	0.010
26	30	4	30	0.43	0.66	3268	2190	0.017
27	30	4	40	0.52	0.8	3879	2920	0.043

5. CONCLUSIONS

In the course of the research, traverse load force F_s* during cutting has been determined experimentally. Dependence of force F_s* on the traverse speed v_t and the string diameter d_s was determined. Dependence of force F_s* on the specified parameters is used in the developed mathematical model describing operation of the installation hydraulic drives.

Main requirements to the installation is to ensure that the deviation of the workpiece's geometric shape does not exceed the permissible values according to the standard, maximum productivity and minimum power losses in the drives.

Major parameters having the greatest influence on the deviation δ have been identified. Dependences of the deviation δ on change in area of the feed hydraulic cylinder f_c, area of the throttle working window f_d and nominal pump pressure p_n have been obtained.

An optimization criterion has been developed for evaluating the installation efficiency including the deviation of the workpiece's geometric shape, the installation productivity, and power losses during its operation.

Based on application of the created optimization criterion, values of the major parameters $f_c=10 \cdot 10^{-4}$ m^2, $f_d=4 \cdot 10^{-6}$ m^2 and $p_n=40 \cdot 10^5$ Pa have been found, at which deviation of the workpiece's geometric shape is $\delta_3=1.88\%$, productivity A = 6258 pcs/h and lost power N = 2920 W.

REFERENCES

1. Adler, Y., Markova, E., Granovsky, Y., (1976). *Planning an experiment when searching for optimal conditions*, Science Publishing House, Moscow.

2. Bushuev, A., Ivanov, M., Korotaev, D., (2018). *Minimization of a mismatch time of movement of actuators of a throttle synchronization system*, Journal of Physics: Conference Series, 1141, doi:10.1088/1742-6596/1141/1/012090.

3. Chen, C., Liu, L., Cheng, C., Chiu, G., (2008). *Fuzzy controller design for synchronous motion in a dual-cylinder electro-hydraulic system*, Control Engineering Practice, 16, 658-673, doi:10.1016/j.conengprac.2007.08.005.

4. Chun-Yu, Z., Yi-Min, Z., Bang-Chun, W., (2010). *Synchronisation and general dynamic symmetry of a vibrating system with two exciters rotating in opposite directions*, Chinese Physics B., 19(3), doi:10.1088/1674-1056/19/3/030301.
5. He, B., Zhao, C., Wang, H., Chang, X., Wen, B., (2016). *Dynamics of synchronization for four hydraulic motors in a vibrating pile driver system*, Advances in Mechanical Engineering, 8(8), 1-15, doi:10.1177/1687814016659043.
6. Jia, Y., Li-jun, Q., (2011). *Hydraulic sheet metal bending machine hydraulic servo valve synchronization systems research*, Second International Conference on Mechanic Automation and Control Engineering, 325-328, doi:10.1109/MACE.2011.5986924.
7. Kassem, S., El-Din, T., Helduser, S., (2012). *Motion Synchronization Enhancement of Hydraulic Servo Cylinders for Mould Oscillation*, International Journal of Fluid Power, 13(1), 51–60, doi:10.1080/ 14399776.2012.10781046.
8. Ke, L., Mannan, M., Mingqian, X., Ziyuan, X., (2001). *Electro-hydraulic proportional control of twin-cylinder hydraulic elevator*, Control Engineering Practice, 9(4), 367-373, doi:10.1016/S0967-0661(01)00003-X.
9. Kozlov, L., Bogachuk, V., Bilichenko,V., Tovkach, A., Gromaszek, K., Sundetov, S., (2018). *Determining of the optimal parameters for a mechatronic hydraulic drive*, Proc. SPIE 10808, Photonics Applications in Astronomy, Communications, Industry, and High-Energy Physics Experiments, 1080861, doi: 10.1117/12.25015280861.
10. Kozlov, L., Polishchuk, L., Korinenko, M., Horbatiuk, R., Orazalieva, S., Ussatova, O., (2019). *Experimental research characteristics of counterbalance valve for hydraulic drive control system of mobile machine*, Przeglad Elektrotechniczny, 104-109, doi: 10.15199/48.2019.04.18.
11. Liu, Y., (2015). *Design on Synchronization Control of Dual-motor in Crane*, Journal of Applied Science and Engineering Innovation, 2(3), 71-73.
12. Miková, L., Kelemen, M., Ujhelský, P., Gmiterko, A., (2014). *The Simulation of Hydraulic Synchronous Lift of Heavy Loads*, American Journal of Mechanical Engineering, 2(7), 191-194, doi:10.12691/ajme-2-7-4.
13. Rafa, A., Yahya, A., Saad, H., (2014). *Theoretical and Experimental Study of Hydraulic Actuators Synchronization by Using Flow Divider Valve*, Journal of Engineering and Development, 18(5), 282-293, doi:10.13140/RG.2.2.11932.95367.
14. Teixeira, P., Vianna, W., Penteado, R., Krus, P., De Negri, V., (2015). *Pressure Modeling and Analysis of a Synchronized Hydraulic Press Brake with Variable-Speed Pump*, Proceedings of the ASME/BATH 2015 Symposium on Fluid Power and Motion Control, FPMC2015-9634, V001T01A067, doi:10.1115/FPMC2015-9634.
15. Wos, P., Dindorf, R., (2015). *Synchronized Trajectory Tracking Control of 3-DoF Hydraulic Translational Parallel Manipulator*, Advances in Intelligent Systems and Computing, 317, 269-277, doi:10.1007/978-3-319-10990-9_24.
16. Yang, Y., Jin, X., (2021). *Simulation analysis of cooperative motion fuzzy control of distributed lifting units*, Journal of Physics: Conference Series., 2087, doi:10.1088/1742-6596/2087/1/012050.

Received: April 20, 2023/ Accepted: December 15, 2023 / Paper available online: December 20, 2023© International Journal of Modern Manucaturing Technologies